

Correspondent: R. P. Johnson
Fermilab

FERMILAB-Proposal-0491

Clashing Gigantic Synchrotrons

C. M. Ankenbrandt, T. L. Collins, H. E. Fisk, R. P. Johnson,
P. Limon, and J. Peoples
Fermi National Accelerator Laboratory

A. V. Tollestrup and R. L. Walker
California Institute of Technology

L. M. Lederman
Columbia University

May 1976

38 pgs.

Table of Contents

	<u>Page No.</u>
I. Introduction	3
II. Creating the Collision	8
A. Beam Reversal	9
B. Luminosity	10
C. Collision Course	13
D. Operation Sequence	16
III. Apparatus	17
A. Impact of Kinematics on Detector Design	17
B. The Detector	18
1.) Drift Chambers	21
2.) Shower Detector	21
3.) Hadron Calorimeter	22
IV. Cross-Sections and Rates	25
A. Rates for W Bosons	26
1.) $pp \rightarrow W^+ + \text{Anything}$	26
2.) $pp \rightarrow W^- + \text{Anything}$	26
3.) $pp \rightarrow W^0 + \text{Anything}$	28
B. Other Physics Rates (Backgrounds?)	28
C. Triggering and Identification	29
V. Expected Future Developments	31
A. Design Improvements	31
B. New Phenomena	32
References	33
Appendix I: The collision Cave	34

I. Introduction

The exciting possibility of arranging collisions between counter-rotating Main Ring and Energy Doubler beams offers a practical and inexpensive first exploration of the TeV center of mass region, a region that was thought to be many years and hundreds of millions of dollars away. A 1000-GeV Doubler colliding with a 400-GeV Main Ring is the equivalent of two beams of 630 GeV each or 1.2 TeV center of mass energy, three times the energy proposed for ISABELLE and more than half that of POPAE. The graph below shows the center of mass energy for various Doubler and Main Ring energies.

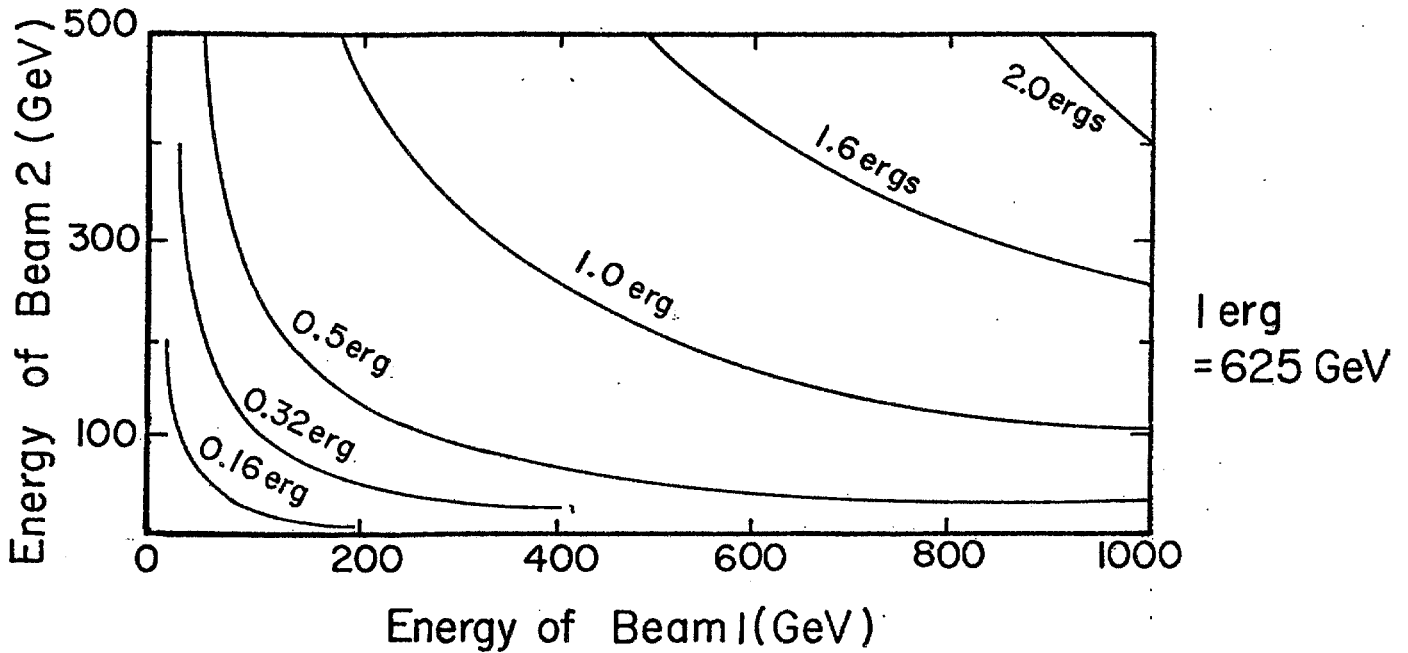


Fig. 1. Center-of-mass energy produced by colliding beams.

Two decades ago the goal of producing the antiproton provided clearcut guidance in the choice of Bevatron energy. Similarly today, the goal of discovering the W, the mediator of the weak interaction, provides a benchmark for comparison of proposed colliding beam facilities. The experiment proposed here has as its main goal the discovery of the elusive W. However, the experimental arrangement will be versatile and sophisticated enough to react to surprises.

The reactions we propose to study are:

- (1) $p + p \rightarrow W^{\pm} + \text{Anything}$
- (a) $\left\{ \begin{array}{l} \rightarrow e^{\pm} + \nu \end{array} \right.$
 - (b) $\left\{ \begin{array}{l} \rightarrow \text{hadrons} \end{array} \right.$
- (2) $p + p \rightarrow W^0 + \text{Anything}$
- (a) $\left\{ \begin{array}{l} \rightarrow e^+ + e^- \end{array} \right.$
 - (b) $\left\{ \begin{array}{l} \rightarrow \text{hadrons} \end{array} \right.$
- (3) $p + p \rightarrow \text{hadrons } (p_T \geq 5 \text{ GeV}) + \text{Anything}$
- $\left\{ \begin{array}{l} \rightarrow \text{high } p_T \text{ correlations.} \end{array} \right.$

The proposal calls initially for 1000 GeV on 150 GeV, corresponding to .77 TeV or 1.2 ergs in the center of mass. At this energy, theoretical calculations based on the Drell-Yan process lead to cross-sections of about 10^{-33} cm^2 or 1 nanobarn for $M_{W^+} = 100 \text{ GeV}$. With this cross-section, the initial design luminosity of $2 \times 10^{30} \text{ cm}^{-2} \text{ sec}^{-1}$ results in a production rate of about 200 W^+ /day as shown in Fig. 2. These calculations are discussed more fully in the following sections.

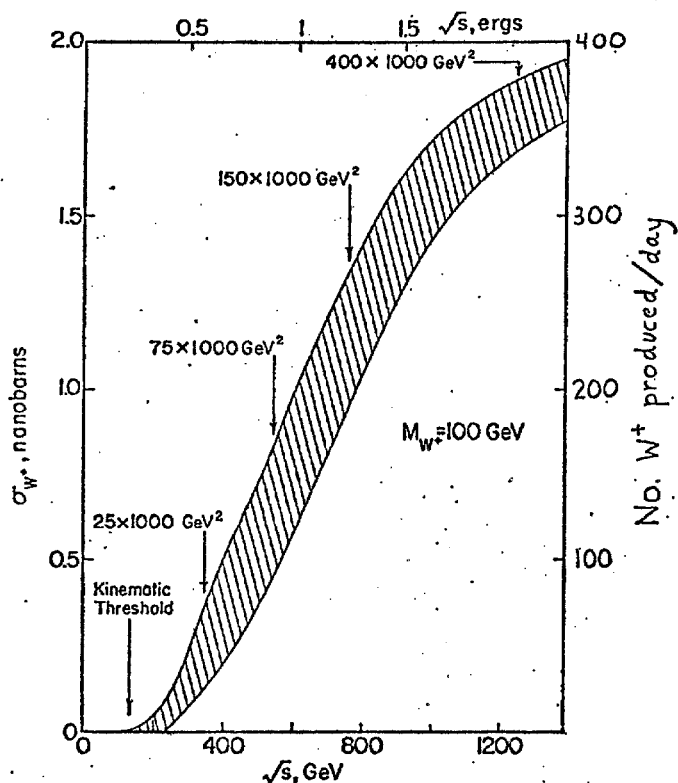


Fig. 2. Cross-sections and rates.

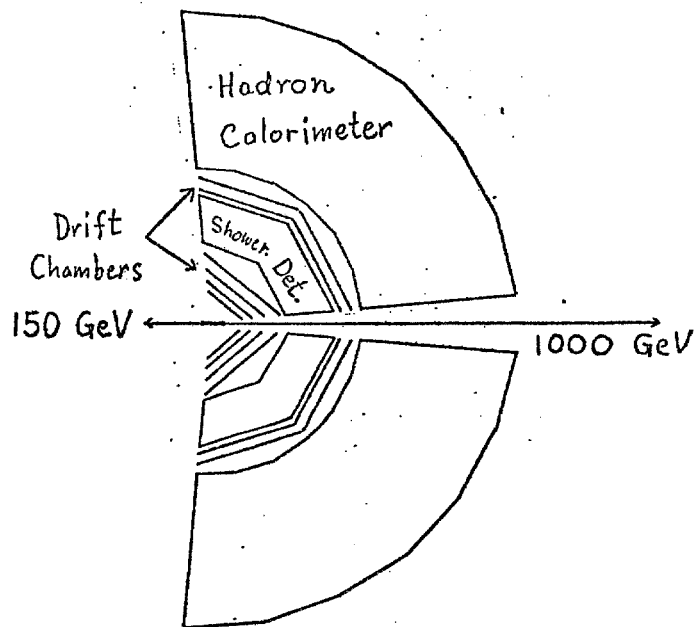


Fig. 3. The detector.

The design of the detector, illustrated schematically above and described in detail in Section III, is enormously simplified by the following two features of the proposed colliding beam scheme:

- (1) The rf will remain on for both beams and hence they will be bunched. This results in an interaction region that is only plus or minus 10-cm long, allowing a small and sophisticated inner detector.
- (2) The asymmetrical collision energies produce a moderate velocity of the center of mass with respect to the lab, resulting in a very convenient lab angular range. For example, for 1000 GeV on 150 GeV, 90° in the center of mass becomes 42° in the lab and a detector subtending the range from 5° to 95° in the lab covers essentially the full range of high p_T phenomena.

In the proposed detector, a particle emerging from the interaction region first encounters a series of track detectors (drift chambers, with 100 μ resolution), then an electromagnetic shower detector (to identify electrons with a hadron rejection factor approaching 10^4), another track detector, and finally a hadron calorimeter. The arrangement has two symmetric arms to carry out the simultaneous study of the reactions (1), (2), and (3) listed above. The apparatus is centered on 90° in the center of mass and subtends the range from about 30 to 120° in this system. Azimuthally, the detector covers $\pm 45^\circ$ in each arm.

The signatures of the reactions of interest are as follows:

W^\pm detection via leptonic decay involves finding a very high p_T ($\approx \frac{M_W}{2}$) lepton accompanied by missing p_T as determined in the opposite side hadron calorimeter. Clearly a reasonable number of events is needed to make this technique convincing.

W^0 detection via electron pair decay is clearly cleaner since a pair signal shows a sharp peak. The apparatus will also look at lower-mass lepton pairs in order to calibrate the W search but the luminosity limit will not permit this to be terribly sensitive, being limited to masses ≤ 10 GeV, far below the expected W mass range.

W^\pm and W^0 detection via hadronic decay has the chief virtue that its rate could easily dominate that of the leptonic mode by an order of magnitude. It depends on the observation of a blast of hadronic matter; e.g., for $M_W = 100$ GeV, perhaps 20 charged particles carrying, on each side, $\frac{M_W}{2} = 50$ GeV of transverse momentum! The hope is that the Σp_T hadronic distribution will peak at $\Sigma p_T = M_W/2$ on each side.

High p_T hadrons. The calorimeter, with moderate resolution, will help sort the hadronic p_T distribution into "charged" and "neutral" correlations; i.e., dihadron "mass" spectra can be studied much as was done in the original ISR experiment of π^0 - π^0 correlations.

The continuum (e.g., "jets" in the parton model) distributions will be important as the background to the $W \rightarrow$ hadron search.

An important feature of the experiment is that either colliding beams or straight-ahead operation is completely programmable. The beams can be brought together at any time up to 150 GeV during a front porch or a flattop and then accelerated further and extracted. This allows the experiment to make operational demands much like any other major experiment, that is, parasitic during tune-up and beam sharing during production.

An additional point to note is that when the Doubler magnet ring is first finished, an experiment such as this may well be the first logical use of the ring while the extraction system and beam lines are being modified to handle the 1000 GeV that will be available.

Finally, we emphasize that this is an opportunity for only a first look at this energy region. It cannot replace a full exploration by a large storage ring facility, but it will be a good look and it can be exciting and fun and provide important guidance on the design of a larger facility. If the W remains elusive then the apparatus will be adaptable to other high transverse momentum experiments. It is important to remember that an energy density of the order of an erg per cubic fermi* is enormous and may produce completely unexpected phenomena, so it would be foolish to be locked into a detection scheme that is not versatile and sophisticated in its design.

* $\sim 3 \times 10^{33}$ BTU/ft³

II. Creating the Collision

A practical arrangement for Main Ring against Doubler colliding beams must satisfy several obvious requirements, namely:

- a) One beam is reversed.
- b) The orbits are brought together.
- c) Beams focus to small size at the collision point to provide adequate luminosity at sensible beam current.
- d) The remainder of the straight section is adequate for the experimental apparatus.
- e) The tunnel is enlarged around the apparatus.

To be really practical it must also be compatible with normal operation of both accelerators. This in turn implies the following constraints:

- a) Reconstruction of the tunnel must be limited to a region comfortably inside the straight-section quadrupoles so that only the vacuum pipe is disturbed. As soon as a (protected) pipe can be re-installed carefully monitored night-time and weekend operation can resume.
- b) The reconstructed tunnel must provide a bypass for regular tunnel traffic (magnet vehicle) which can be kept clear even during assembly of the experiment.
- c) The arrangement must not compromise operation of either accelerator. In particular the Main-Ring beam should be completely unaffected when the experiment is off.
- d) The program demands of the experiment must resemble those of other major experiments: parasitic during tune-up, beam sharing during data taking, and capable of fully utilizing the accelerator if it is made available.

We present herein our most conservative arrangement which satisfies all these requirements. This arrangement presumes no technical developments except satisfactory operation of the Doubler as an accelerator with a long flattop; even so the colliding beam performance specifications are impressive:

Main Ring energy	150 GeV
current	2×10^{13} protons (present value)
Doubler energy	1000 GeV
current	2×10^{13} protons (no stacking)
Center-of-mass energy	.77 TeV (385 on 385 equivalent)
luminosity	$2 \times 10^{30} \text{ cm}^{-2} \text{ sec}^{-1}$

Flexibility: complete, collision and focussing can be programmed on and off with beams in the accelerators.

A. Beam Reversal

We choose to reverse the Doubler during experimental operation. Later, when the demand for external Doubler beams has increased we can move the apparatus and modify the operation cycle, but in the meantime the output of the Main Ring will be normal. (A reversed Doubler has other very attractive uses and may be quite popular.) The design of injection into and operation of a reversed Doubler presents no problem. Reverse injection into and operation of the Main Ring to 100 GeV is required.

The conservative easy-to-design way to inject backwards into the Main Ring starts with a new Booster extraction 130° upstream of the present one. After matching, the beam is transported directly across country, outside the Main Ring, to medium straight section F. This

transport is 2000-feet long, but consists only of a vacuum pipe buried below the frost-line with small manholes every hundred feet for small air-cooled quads ($\int Gdl = 12$ kilogauss). A hole drilled in the Main-Ring tunnel roof provides entry. Injection at a medium straight is easy and no holes in magnet cores are needed.

Other methods for injecting the beam from the Booster into the Main Ring in the backward direction are also being considered.

Reverse operation of the Main Ring primarily requires remotely-operated reversing switches on the power supplies. Both the quad and bending magnet currents must reverse so that the maximum beam height remains in the large gap B2 magnets. The only other addition is a 100-GeV reverse path into the abort dump; all other equipment, particularly the rf, is unaffected by beam direction. After the computer has been taught new tricks the complete cycle, producing one reverse acceleration and return to normal (with a quick empty run to 400 GeV to reset the remanent field), will take less than 1 minute.

B. Luminosity

Luminosity calculations start with an estimate of the beam size in the accelerator. We follow the recommended formula for Main Ring emittance ϵ ,

$$\epsilon_v = \epsilon_h = (.1 n/E) \text{ mm-mrad}$$

where the beam is $n \times 10^{13}$ protons of energy $E(\text{GeV})$. This formula reflects the observed growth of the beam size with current as well as the similarity of horizontal and vertical size. The full beam size at a point with focussing parameter β (meters) is $2(\epsilon\beta)^{1/2}$ mm. One normally assumes Gaussian beam shapes, not because the beam is

precisely that shape but because it is much closer to Gaussian than to rectangular, which is the other shape with easy arithmetic. The Gaussian rms width σ is given in our case by

$$\sigma^2 = \epsilon\beta/6 \text{ mm} = .01 \text{ n}\beta/6E \text{ cm.}$$

We want head-on collisions between bunched beams because the short interaction region greatly improves the experiment. In that case the luminosity

$$\mathcal{L} = \frac{n_1 n_2 \times 10^{26} f_0}{2\pi h} \left(\frac{1}{\sigma_1^2 + \sigma_2^2} \right)$$

where $n \times 10^{13}$ protons are in h bunches with revolution frequency f_0 . One can see the development of this formula as follows: suppose that beam two is very small, $\sigma_2^2 \ll \sigma_1^2$. The luminosity is simply the particle current in that beam ($n_2 f_0$) times the density it encounters in the other beam. The other beam has n_1/h particles in a bunch which multiplied by $1/2\pi\sigma_1^2$ gives the central density for its double Gaussian cross-section. The addition of σ_2^2 , as above, is correct for any size. Inserting proper values

$$\mathcal{L} = 7.44 \times 10^{26} \frac{n_1 n_2}{\sigma_1^2 + \sigma_2^2} \text{ sec}^{-1}.$$

An obvious way to increase the luminosity is to reduce σ^2 by focussing the beam to lower β . A very easy and practical low beta for a main-ring straight section can be achieved by simply powering the present quads in that straight section from three separate, programmed power supplies.¹

The important properties are:

- a) Beta at the center of the main-ring long straight section is reduced to 2.5 meters (70 meters is normal).
- b) Continuous adjustment is possible with beam in the accelerator.

- c) Starting normally and adjusting the quadrupole currents as the energy increases keeps the maximum beam size (in one of the quads) smaller than the injection size.
- d) A small adjustment of the regular quad current keeps the tune constant with very small beta change in the rest of the machine.
- e) The off-momentum displacement $\eta \Delta p/p$ is almost zero, at the center.
- f) Nothing is added to or removed from the tunnel and no straight section space is lost.

These highly desirable properties are obtained up to 155 GeV. Above this energy some of the quads are driven too hard for continuous operation and beta must be returned to normal. This limitation is reflected in our conservative parameter list. Further design may allow small β and large luminosity at higher Main-Ring energies.

The Doubler beta can also be lowered in one or more straight sections. Doubler superconducting quads are much stronger than the Main Ring quads, allowing shorter quads and longer bends. In the present Energy Doubler design there are places to add quadrupoles. If some of these spaces are filled one can obtain a 28 m beta at the center instead of 70 m. This design has not been investigated in detail.

The momentum spread in a Main-Ring beam is also approximately Gaussian. A value of .1 ev-sec is generally used for the emittance (in longitudinal phase space), although measurements usually give a small value. Converting to $\Delta p/p$ and bunch length one finds, with no acceleration

$$\sigma_p = 3.6 \times 10^{-3} v^{1/4}/E^{3/4}$$

$$\sigma_\ell = 44 / (v^{1/4}/E^{1/4}) \text{ cm}$$

for a beam bunched by v MeV/turn. When two bunched beams with the same σ_ℓ collide head-on the interaction region is a Gaussian shape with length $\sigma_\ell/\sqrt{2}$.

The tune shift for a proton with small betatron amplitude in beam 1 is given by

$$\Delta\nu_1 = 6.2 \times 10^{-4} (E_2\beta_1)/(E_1\beta_2)$$

for beams following the current-emittance rule given above. A value $\Delta\nu = .005$ is considered quite safe.

Table I summarizes the luminosity calculations. Note that the momentum width and tune shifts are negligible. An increase of beam current in the Main Ring and Doubler would increase the luminosity. Multiturn stacking in momentum space in the Doubler would also increase the luminosity essentially proportionally until the momentum width became significant (10-20 batches). The luminosity will start at least at 2×10^{30} and should increase to several $\times 10^{31}$.

C. Collision Course

Bringing the beams together in the straight section is not trivial, even with the Doubler moved to its present position 18" directly below the Main Ring. New schemes are to be compared to our standard described below which has the following properties:

- a) It works easily up to 150 on 1000 GeV.
- b) It leaves 5.0 m absolutely clear on each side of the interaction.
- c) It is completely flexible in operation, it can be programmed on and off with beams in the accelerators.

- d) It uses normal magnets in their natural form, a narrow gap with a wide pole face.

The scheme uses four laminated steel magnets to create a typical 4-magnet bump, mostly on the 150-GeV beam. (The magnets would probably split into 8 for handling.) Allowing for coil ends one needs 21 kG for 150 GeV Main Ring on 1000 GeV ES/D.

Table I - Colliding Beam Parameters

	Main Ring	Doubler	Units
Energy	150	1000	GeV
Intensity	2×10^{13}	2×10^{13}	
Interaction β	2.5	28	Meters
η	.14	.28	Meters
$\sigma_h = \sigma_v$.023	.030	cm.
$\eta \sigma_p$.0015	.0005	cm.
RF volts/turn	3	.45(?)	MeV/turn
σ_p	1.1×10^{-4}	$.17 \times 10^{-4}$	
σ_ℓ	9.6	9.6	cm.
Tune shift	.0004	.0010	
90% interaction length		22	cm.
Luminosity		2.0×10^{30}	cm. ⁻² sec. ⁻¹

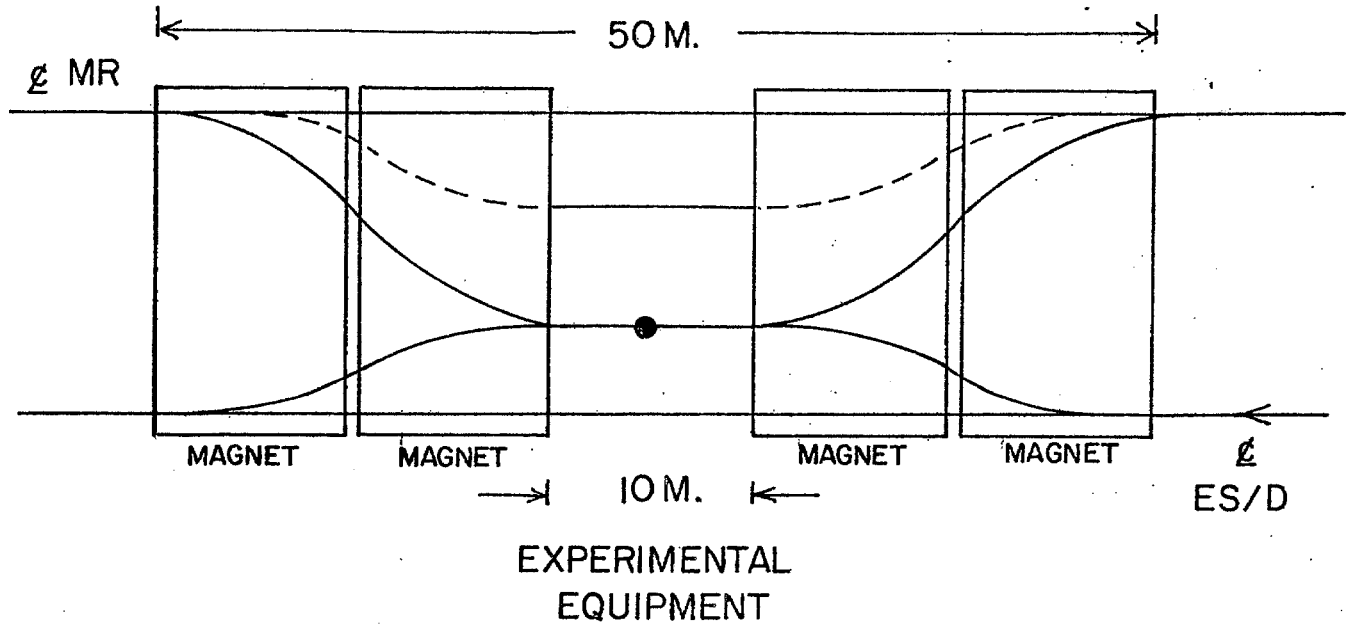


Fig. 4. Configuration of the long-straight section for colliding beams.

The poles span both beams from undeflected beamline to collision, and a wide common vacuum chamber 4" x 20" allows complete programming flexibility.

Trim coils or differential power supplies provide complete vertical steering control. In particular this control must provide a small angle ($\alpha < 1$ mrad) at the crossing to avoid collisions at the next bunch points and consequent background in the experiment. Because the bunch length is so short, the head-on luminosity still is essentially correct, the correction factor being $1 - .1 (\alpha \sigma_{\ell} / \sigma_v)^2$.

D. Operation Sequence

The following sequence presumes the initial arrangement with the Doubler reversed:

- a) A reverse injection into the Doubler via the Main Ring is initiated. Less than 1 minute later the Main Ring is again accelerating normally. This procedure will be repeated according to the Doubler storage time. The interval will certainly be longer than 1 hour. The Doubler beam must be safely dumped at the end of its useful life.
- b) Many Main-Ring pulses are accelerated. Injection and extraction always use a normal machine with the collision course and low-beta off. The program varies from just touching the beam on the fly for tune-up studies, to a full flat-top of a minute or more at 150 GeV when hot W results are coming in. Normal data taking would use a front porch followed by acceleration and normal extraction. The length of the front porch would be negotiated because it does slow the cycle for other experimenters.

III. Apparatus

A. The Impact of Kinematics on Detector Design

An advantage of collisions of two beams of unequal energy is the moderate velocity of the center-of-mass system in the lab system. Table II shows some kinematical examples. If W's are produced at

Table II - Kinematic Examples

E_1	E_2	β_{cm}	γ_{cm}	$\theta_{Lab} (\theta_{cm}=90^\circ)$	\sqrt{s}
400 GeV	25 GeV	.88	2.12	28°	200 GeV
"	50	.78	1.59	39°	282
"	150	.454	1.12	63°	490
1000 GeV	25	.95	3.24	18°	316
"	50	.90	2.34	25°	447
"	150	.74	1.49	42°	775

relatively small x as suggested by past experience with other particles as well as by Drell-Yan type calculations of W production, then their decay products are emitted at very convenient laboratory angles. Figure 5, for example, shows the momentum-angle correlation for electrons from the $e\nu$ decay of W's produced at various x values for 150 GeV on 1000 GeV. These convenient lab angles, together with the small interaction region, result in the compact detector design illustrated in Fig. 6 (a,b). This detector covers half the azimuthal angular range ($\pm 45^\circ$ on each side) and the polar range $30^\circ \lesssim \theta_{cm} \lesssim 120^\circ$. The design is modular to allow easy assembly as well as rearrangement in response to experimental needs or different combinations of energies of the two beams.

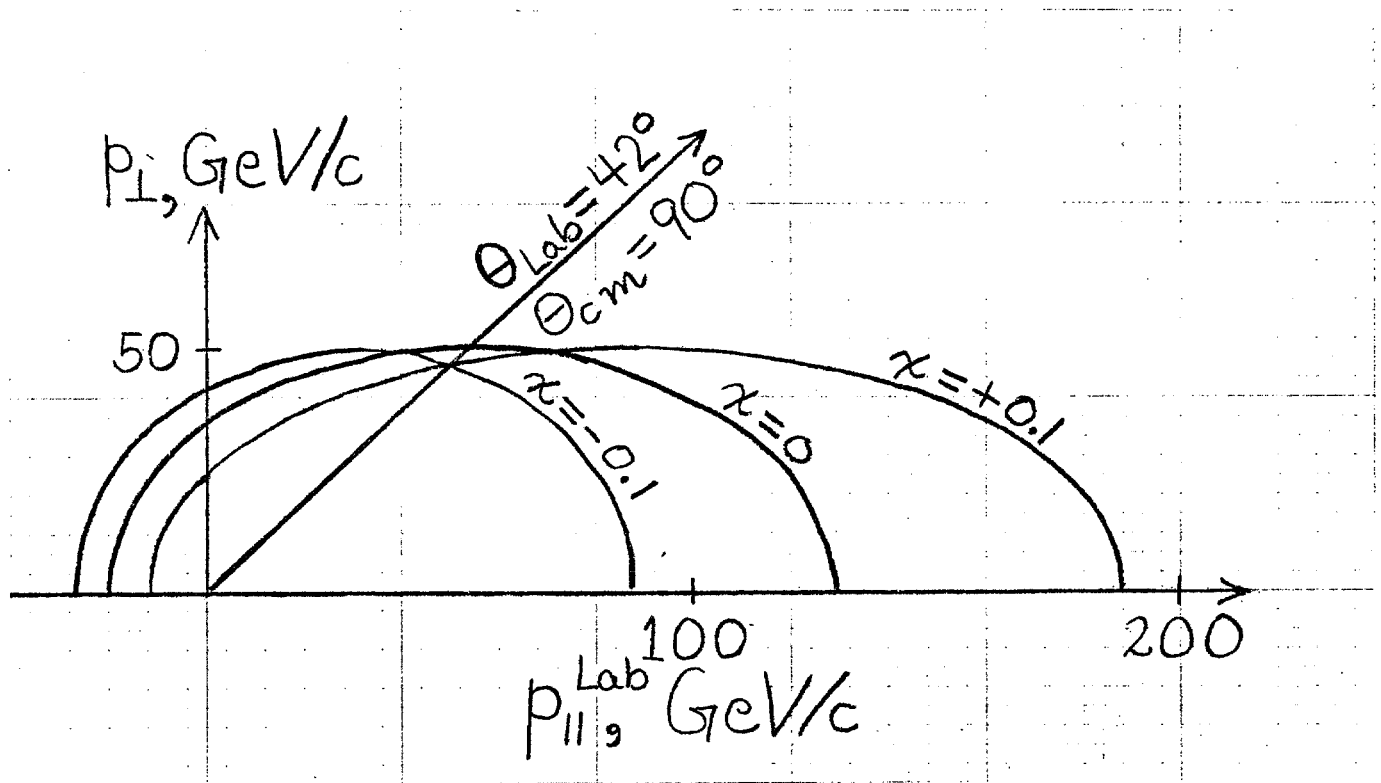


Fig. 5. The laboratory momentum-space Peyrou plots for electrons from $W \rightarrow e\nu$ (or ee) decay. The electrons arise from 100 GeV W 's produced at the indicated Feynman x with $p_T = 0$ in $150 \times 1000 \text{ GeV}^2$ collisions.

B. The Detector

The detector is sensitive to $W^\pm \rightarrow e^\pm \nu$, $W^0 \rightarrow e^+ e^-$, and $W \rightarrow$ hadrons, all at high p_T . It makes use of drift chambers, electromagnetic shower detectors, and hadron calorimeters. Although the details of the design are preliminary, this combination of techniques seems to offer the most information, the best background rejection, and the flexibility to optimize the experiment in response to interesting physics results.

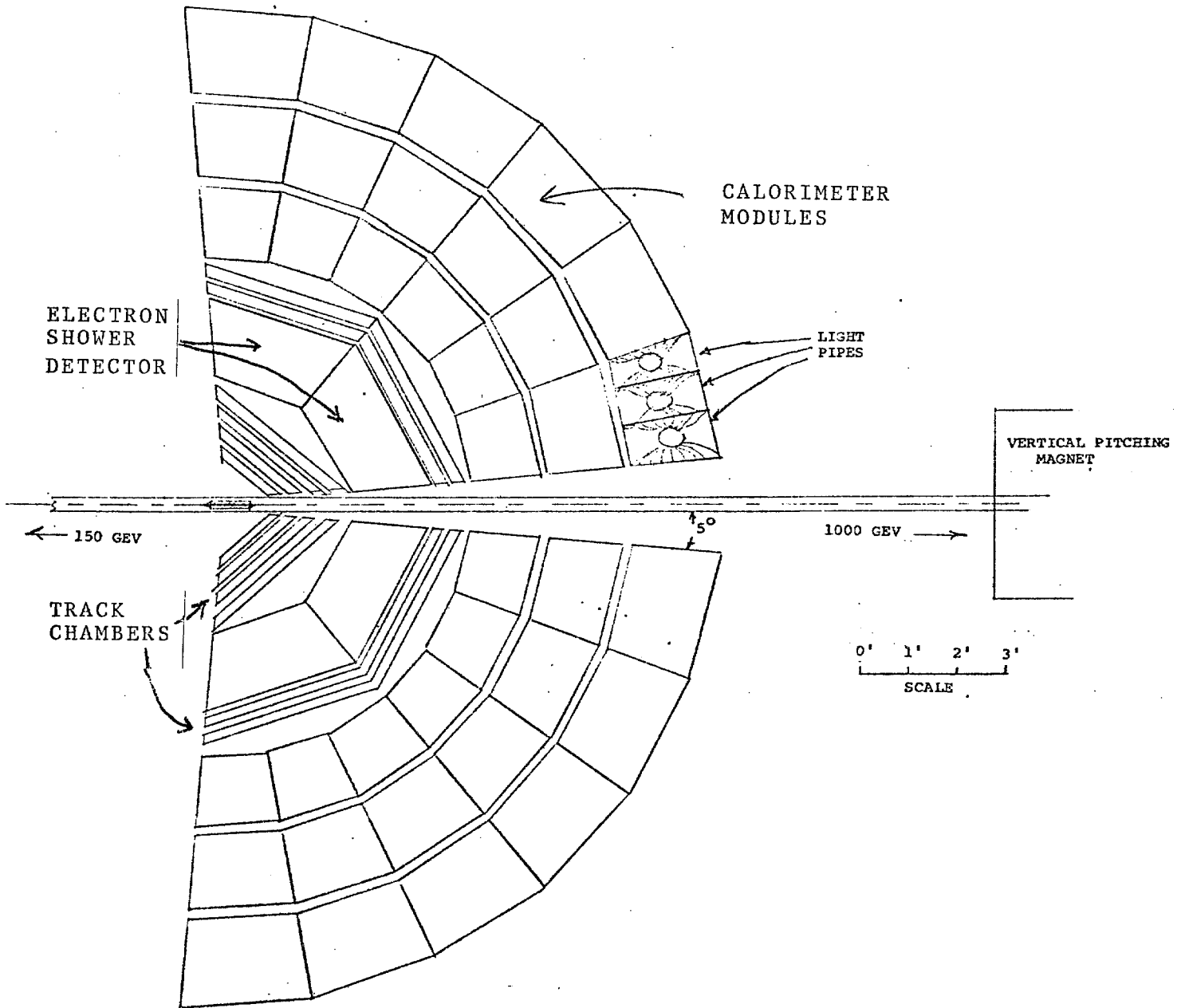


Fig. 6(a). Plan view of the detector.

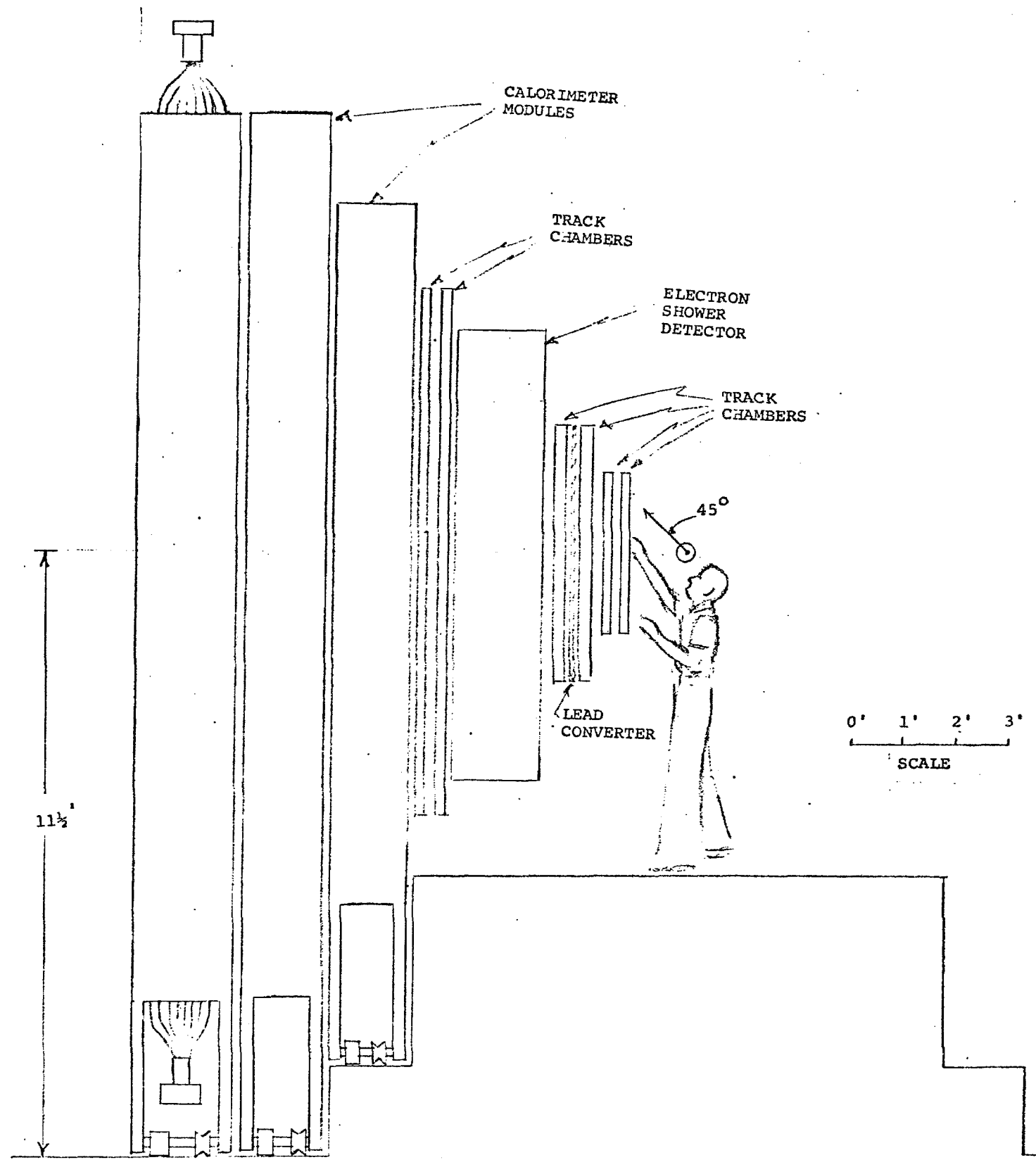


Fig. 6(b). Elevation view of the detector.

1. Drift Chambers

The drift chambers serve to measure track angles accurately and to augment the calorimetry by locating the trajectories of individual charged particles.

The electronic time digitizers recently designed and constructed at Nevis permit digitizing drift times in ≈ 1 ns bins to realize the intrinsic chamber resolution of less than 100 μm . They are capable of handling many hits per wire. The tight time structure of the interactions due to the rf bunched beams simplifies the determination of drift times.

2. Shower Detector

We have considerable experience in lead glass Cerenkov spectrometers and in high spatial resolution converter-scintillation hodoscope spectrometers.² Both have been used extensively to study electrons and photons in a high hadronic background. Here we need to push to more detailed study of the electromagnetic shower development in order to achieve hadron rejection factors of $\sim 10^{-4}$. The expectation, extrapolating from ISR energies, is that $e/\pi \sim 10^{-4}$ and it would be elegant to have a single arm capability at this level. The electromagnetic calorimeter requires good spatial resolution to distinguish closely correlated hadrons and photons and to permit a study of the transverse shower development. Additional rejection is obtained by studying the details of the rapid rise in ionization between thin lead converters in the front and from the absence of any hadronic residue after ~ 30 rad lengths.

Intrinsic backgrounds to searches for $W \rightarrow e\nu$ are Dalitz and external conversions of π^0 and η^0 gammas which, at ISR energies, tend to levels near 10^{-4} and can be sensitively subtracted by extrapolation of a converter curve. The hadron leakage can be studied by absorbing the photon-electron component (it takes only 2 inches of Pb!). (The alternative, muon detection, would require a study of the spectra of pions and kaons and a variable density absorber whose placement is limited by the vacuum chamber.)

3. Hadron Calorimeter

Since the leptonic branching ratio of W bosons is uncertain, the detector includes hadron calorimetry to detect W's by measuring the transverse momentum of their hadronic decay modes. The calorimeter also aids in the identification of electrons and in the selection of events in the trigger. The scintillators are grouped into modules in the polar angle coordinate, and have photomultiplier tubes at each end, permitting vertical spatial resolution by pulse height and timing. The geometry can also be changed with relative ease, to allow for the various possible energy configurations and circulating beam directions of the ES/D and the Main Ring.

Although we have not yet decided the type of calorimeter to use, we present a possible design for a steel-scintillator sandwich, since there are considerable data available for that type of design.³ It is known from existing data that it is important to absorb as much of the hadronic shower as possible. At 10 GeV, 99% of the shower is absorbed in 90 cm of steel; at 300 GeV, 99% is absorbed in 130 cm of steel. A counter of about 120 cm depth is then adequate for the

expected range of energies. A reasonable compromise between resolution and cost consists of 2-inch thick steel plates separated by .25-inch plastic scintillator. This results in a total thickness of the calorimeter of about 5 feet, with 24 layers of scintillator. The light from the scintillator is collected by light pipes which connect the vertical slats along the depth of the calorimeter. If we build the calorimeter in modules of a few interaction lengths each, we can get valuable information about the shower development, and also make the whole array easier to handle. With a geometry of this type, an rms resolution of 15% at 30 GeV is standard, decreasing to 8% at 100 GeV.

The counters are quite long, particularly those in the back. For these modules it may be preferable to use liquid scintillator, which has better light transmission than plastic, and is considerably less expensive. The calorimeter would get slightly larger in that case, requiring more steel. Another possibility is the new doped Lucite type of scintillator. Although the light output is less for the doped Lucite, we will have more than enough light, and will probably have to throw some away to keep within the dynamic range of the phototubes.

The modules are supported on rails, which form semicircles centered on the interaction region. If the beam energies are changed, each module can be moved along the rails into a new position. The drawing shows the counter covering a range in polar angle from 5° to 95° as appropriate for beams of very unequal energy. For equal energy beams, or antiprotons on protons, the apparatus would be swung around to cover $\pm 45^\circ$. If the beam directions are reversed, so that the other accelerator can extract beam to the Experimental Areas,

the apparatus can be moved to cover the other hemisphere. The largest module is about 16 tons, and the whole apparatus weighs 400 tons. This modular design allows us to include as many modules as are practical and useful. In particular, we could split the units to put some in the backward direction, or move them away from the forward direction if the noise is too high there. Furthermore, interesting physics can begin before all modules are in place. In short, we put detectors where they are most useful.

The vertical spatial resolution from timing alone should be about 8 inches. Each module is segmented to have a comparable horizontal resolution. The final resolution is determined by the track chambers, of course, and the only problem that arises because of the spatial resolution of the calorimeter is the possibility of more than one hit within the resolution of the counter. This is not expected to be a problem.

IV. Cross-Sections and Rates

Cross-section calculations for intermediate vector boson production from pp collisions are usually based on the Drell-Yan mechanism.⁴ In this model a quark in one proton and an antiquark in the other annihilate to produce the W boson. The major uncertainties in the calculation are the fraction and momentum distribution of the antiquarks in the proton. Experimentally, the antiquark momentum distribution can be measured with deep inelastic lepton-nucleon scattering. At present, the results are not as good as might be hoped, but the presently acceptable distribution is thought to be between a) $x\bar{q}(x) \propto (1-x)^7$ and b) $x\bar{q}(x) \propto (1-x)^{7/2}$. Here x is the Feynman variable $x = p_{//} / p_{// \text{ max}}$. Cross-sections displayed below will be for these two \bar{q} distributions.⁵

The existence of the Drell-Yan mechanism can be tested experimentally by measuring the pp cross-section to produce massive lepton pairs. At large masses the dileptons should be produced primarily by this mechanism. Preliminary measurements at Fermilab⁶ indicate that the Drell-Yan mechanism agrees with the data only if another internal degree of freedom (color) is assumed to exist for the quarks. This is consistent with the present quark picture in which, for example, the $\pi^0 \rightarrow \gamma\gamma$ rate is correctly predicted with colored quarks.

The Fermilab data, which are amazingly close to the predictions, do not prove the existence of the Drell-Yan mechanism. They do at least imply that a colored quark model must be used. And, although the predicted rates are thus lower by 1/3, all rate discussions are

based on colored quarks.

A. Rates for W Bosons

1. $pp \rightarrow W^+ + \text{Anything}$

Figure 7 shows the pp cross-section to produce a 100 GeV W^+ boson as a function of total center-of-mass energy. This cross-section at $\sqrt{s} = 770$ is calculated to be between 1.0 and 1.3×10^{-33} cm² for the two \bar{q} distributions above. The rate for interactions is then $r = \mathcal{L}\sigma \cong 2.3 * 10^{-3} \text{ sec}^{-1}$.

The detected event rate will depend on the solid angle subtended by the detector ($\sim 1.2\pi$ sr), the machine duty cycle (taken to be 1 for production runs), the hadronic branching ratio (~ 0.8) and the $e\nu$ branching ratio (~ 0.1). One could also imagine a factor for the decay angular distribution, but the W should be produced at low x and an isotropic or nearly isotropic decay is most likely. The rate to see a single electron or a hadron jet from the W decay is

$$r = 2.3 * 10^{-3} \left(\frac{1.2}{4} \right) (.9) = 6.2 * 10^{-4} \text{ sec}^{-1} \\ \cong 2.2/\text{hour} \cong 53/\text{day}.$$

The rate will be further reduced by some as yet unknown amount due to fiducial volume cuts and trigger and identification efficiencies. Something in excess of 10 detected events/day seems a conservative estimate.

2. $pp \rightarrow W^- + \text{Anything}$

Since there is as yet no way to measure the charge sign of the produced boson in the proposed detector, the W^- signature will be identical to the W^+ . Due to the quark structure of the positive proton, the $pp \rightarrow W^-$ cross-section is lower than that for W^+ by a factor of 1/3 to 1/4 for a mass of 100 GeV and $\sqrt{s} = 770$ GeV.

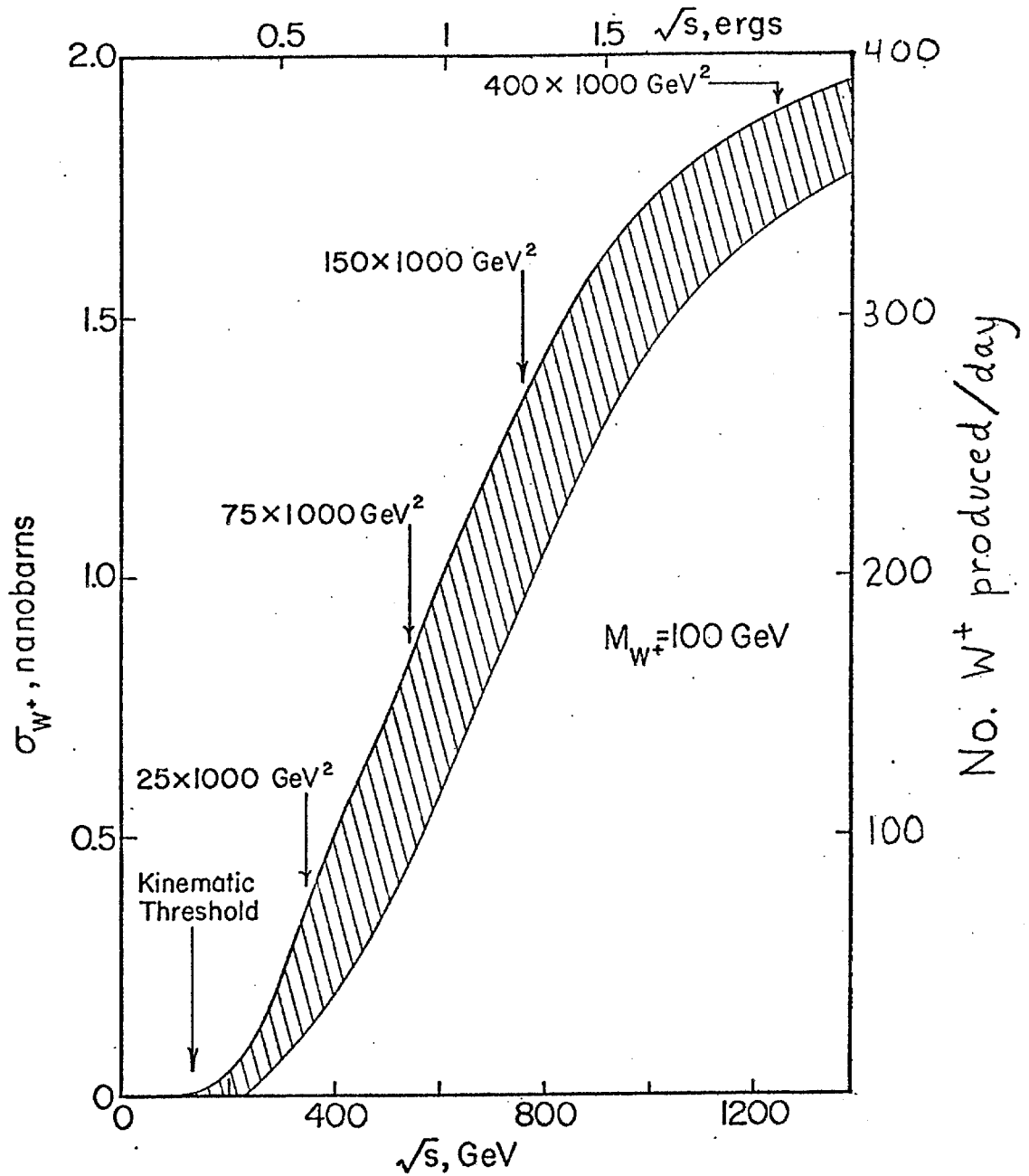


Fig. 7. Cross-sections for $pp \rightarrow W^+ + \text{Anything}$, adapted from unpublished calculations of C. Quigg. The shaded band lies between extreme parameterizations of $\bar{q}(x)$. The upper curve results from $x\bar{q}(x) \propto (1-x)^{7/2}$ a'la Pakvasa et al, the lower curve derives from $x\bar{q}(x) \propto (1-x)^7$ a'la R. Field.

3. $pp \rightarrow W^0 + \text{Anything}$

The predicted rates for the mediator of the weak neutral current depend on the value of the Weinberg angle. For $\sin^2 \theta_W \sim .3$ to $.4$, the W^0 cross-section is lower than the corresponding W^+ cross-section by about a factor of $1/2$.

B. Other Physics Rates (Backgrounds?)

There may be other interesting scalar or vector mesons produced in pp collisions at energies above 100 GeV in the center of mass, such as Higgs Scalars, etc.

One would not normally consider new phenomena to be backgrounds but there may be other types of interactions which make it difficult to detect the production of W's. The basic mechanism for making a W^+ is assumed to be quark-antiquark annihilation:

e.g.
$$u + \bar{d} \rightarrow W^+.$$

Background from quark-quark scattering must be estimated. Using phenomenological models for the quark longitudinal momentum distributions, the "blackbox" $q + q \rightarrow 2$ hadron jets cross-section has been estimated at 90° in the center of mass. It is believed to be down more than a factor of two from that expected in W^+ production for W^+ mass of 50 GeV.⁷ This background is reduced about two orders of magnitude if the W mass is 100 GeV.

Two additional sources of quark-quark scattering are photon and W^\pm exchange. Background estimates for these two processes are more reliable and lead to the conclusion that these backgrounds will be down by two to three orders of magnitude at 50 GeV.

Observing hadrons produced at 90° in the center of mass is in itself very interesting physics and even if such background exists it will be possible to see a decent signal from W^+ production since the transverse momentum of the decay products must add to give the mass of the W boson and thus cut off at some p_t . Of course the leptonic decay modes are not directly obscured by these hadronic processes.

C. Triggering and Identification

1. Event Selection in the Trigger

The event selection will be the logical sum of various simple requirements on transverse momentum. The detector is segmented and it will be easy to form cells of production angle intervals about some angle θ such that the products $E_{\text{shower}} \sin \theta$ and $E_{\text{hadron}} \sin \theta$ for each cell are available to form sums and/or correlation requirements. The proper thresholds will be determined in situ.

The reactions of interest can be selected in the trigger by the following requirements:

- 1.) $W^\pm \rightarrow e^\pm \nu$: high electromagnetic p_T on one side;
- 2.) $W^0 \rightarrow e^+ e^-$: high electromagnetic p_T on both sides;
- 3.) $W \rightarrow \text{hadron}$: high hadronic p_T on both sides;
- 4.) High p_T phenomena: high hadronic p_T on one side.

2. Isolating the W Signal

The neutrino carries off transverse momentum in the leptonic decay of the W^\pm . Thus, the calorimeter on the side opposite the detected electron will be used offline to verify that transverse momentum is missing.

The electron pair decay mode of the W^0 will be the most obvious and convincing boson signature, since the pair mass can be reconstructed. However, the rate may be low.

The W hadronic mode is detected by a coincidence between the two arms of the spectrometer. There will be a blast of hadronic matter with enormous transverse momentum in each arm. For $M_W = 100$ GeV there might be 20 or so particles carrying a total of about $\frac{M_W}{2c} = 50$ GeV/c of transverse momentum on each side. To the extent that the detector observes all the transverse momentum, the sum of the transverse momenta will peak at the mass of the boson.

V. Expected Future Developments (Work in Progress)

A. Design Improvements

Schemes to improve the luminosity are being actively pursued. Additional quadrupoles added to the ends of the MR straight sections might be used to keep the machine β function low at higher MR energies than 150 GeV.

The magnets used to bring the beams together in the long-straight section are yet to be detailed. Perhaps with the use of superconductivity, a more compact magnet would allow a longer free space for the experimental detector. From another point of view, it seems possible that these "combining" magnets could be incorporated into the experimental design. Namely, an enlarged field region could extend over the interaction and provide momentum analysis for the reaction products.

The possibility of stacking beams in the ES/D to improve the luminosity and the problems of subsequent beam instabilities are being investigated.

Improvements to the detector are being considered which would improve the detection solid angle as well as add momentum determination and muon identification. The solid angle in the forward direction can be covered by counters close to the beam pipe.

The interaction vertex position transverse to the beam direction will be known extremely well due to the low β value of the MR (the interaction cylinder is less than 1 mm in diameter). Two properly placed drift chambers and a short solenoidal field could be used to measure outgoing momenta to good precision in a few feet. The

momentum knowledge would help in the electron vs. pion identification in the shower counter as well as provide the transverse momentum of muons. The muon is identified by passing unscathed through the shower and calorimeter converters after its momentum (or lower limit on its momentum) has been determined.

B. New Phenomena

The development of the detector depends upon the imagination of the experimenters. Detectors, triggers and even methods of analysis depend on expectations. We will try to expand the concept of our general purpose detector to anticipate as much as possible the existence of entirely new phenomena.

For example, the shower detector may be made as large as possible to detect multiphoton events (e.g. Schein events or magnetic monopoles). Perhaps ionization can be measured in case quarks can, after all, escape from a nucleon.

There is no doubt that the thing most worthwhile to discover is that which has not yet been imagined.

The enormous energy available in MR-ES/D collisions is almost a guarantee that our view of the universe will be expanded. Let us get on with it.

References

1. T. L. Collins, "Easy Low Beta for the Main Ring,"
TM-649 0400, March, 1976.
2. R. P. Johnson et al, Nuclear Instruments and Methods, 120
(1974) 391. L. M. Lederman et al, Fermilab Experiments 70,
288. A. V. Tollestrup, R. L. Walker et al, Fermilab Exp. 111.
3. See, for example, The Proceedings of the Calorimeter Workshop,
Fermilab, May, 1975.
4. Sydney D. Drell and Tung-Mow Yan, Phys. Rev. Letters 35, 316
(1970).
5. We would like to thank Chris Quigg for enlightening discussions.
6. Private communications from anonymous participants of Fermilab
experiments E70, E288, and E325.
7. Rick Field - private communication.

Appendix I: The Collision Cave

A design for a suitable experiment space is shown in Fig. 8-10.

The design has the following features:

- a) The design fits any unmodified straight section. For example, there is little difference between D0 and E0, except that it is much easier to provide good drainage at D0. The major vehicle access at D0 (off the lower left corner of the drawing) is unaffected by construction.
- b) The basic experiment floor space is ± 16 feet along the beam line and ± 12 feet transverse. This 32×24 ft² area is a pit whose floor is 11.5 ft below beam height and is contained in a 32×48 ft² structure with the longer dimension transverse to the beam.
- c) A bypass for tunnel traffic occupies 6 feet. Two extra loops must be replaced on each side to make a passage that the magnet vehicle can negotiate. The existing tunnel to the service building stairs connects to this traffic-way.
- d) Installation of the apparatus is a big job. It will occur during every possible tunnel access, but it must not interfere with Main Ring maintenance or Doubler installation by blocking free flow of tunnel traffic. For this reason a separate access for heavy experiment components is provided at the backend of the structure. This area has an elevated floor which make a simple truck ramp very practical. A movable bridge is placed across the beam pipe from this area to the traffic-way.

- e) The closest machine components (quads) are 43 feet from the construction and will not be disturbed. The construction region contains only a vacuum pipe which can be replaced shortly after excavation allowing carefully monitored Main-Ring operation outside of construction hours.
- f) The present utility building can house power supplies and cooling equipment for the collision magnets and low beta system. A duct bank to the upper corner of the structure provides a very direct data path between the experiment Porta-kamps and the apparatus.
- g) Once the collision cave is substantially complete there will be no interference by experiment installation, with operation and maintenance of the Main Ring or with commissioning of the Doubler.

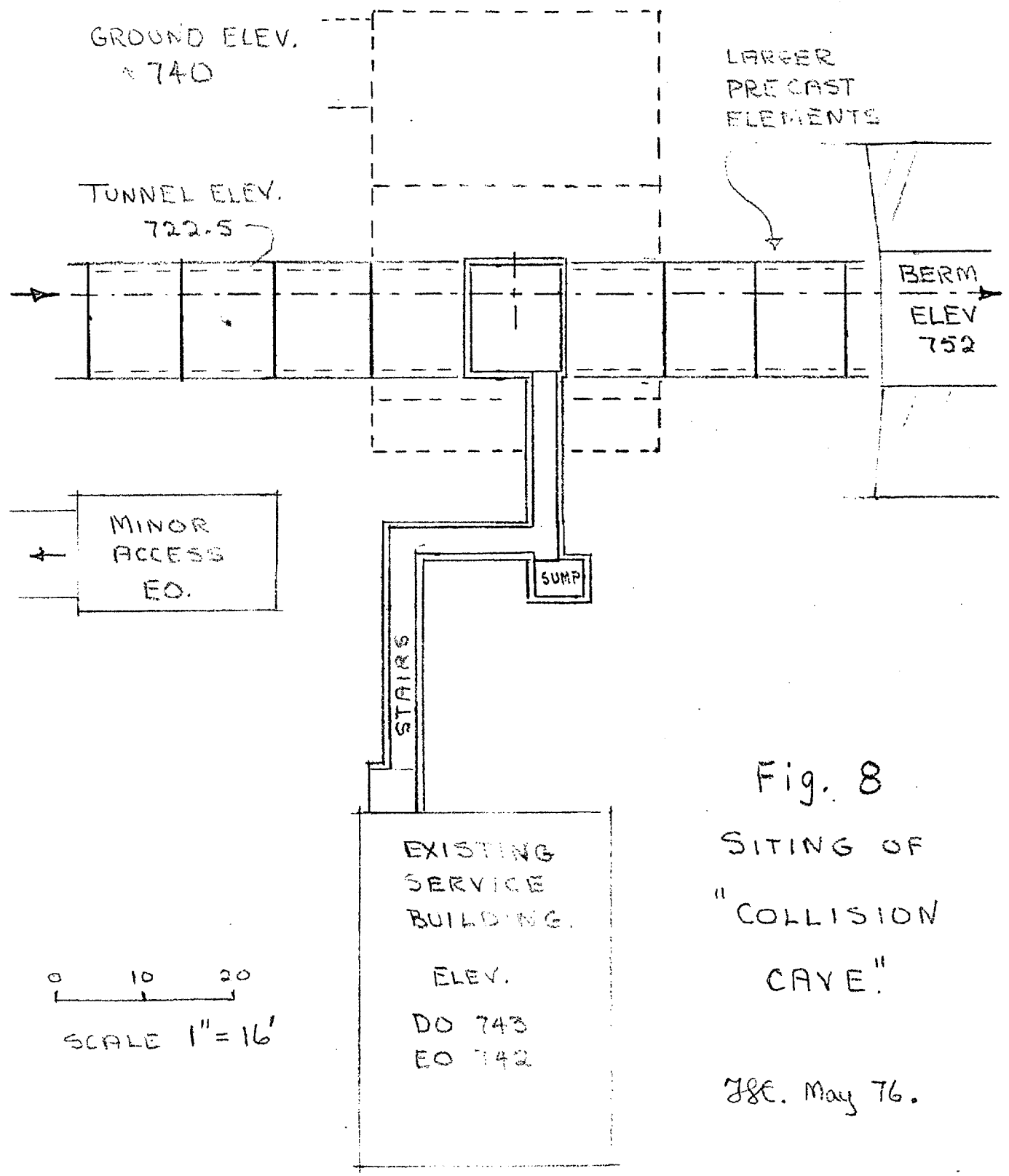
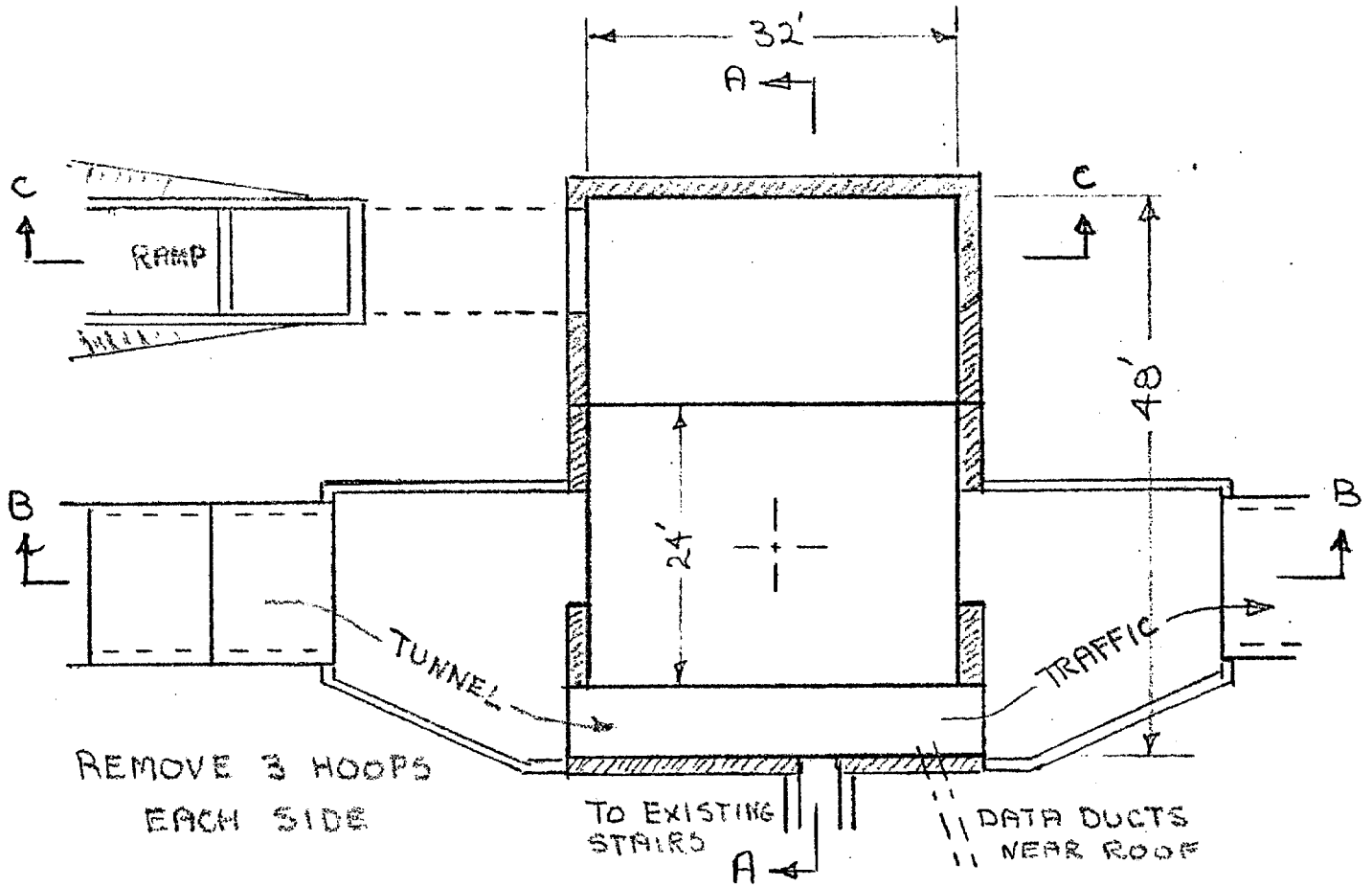


Fig. 8
SITING OF
"COLLISION
CAVE"

J&E. May 76.



SECTION A-A

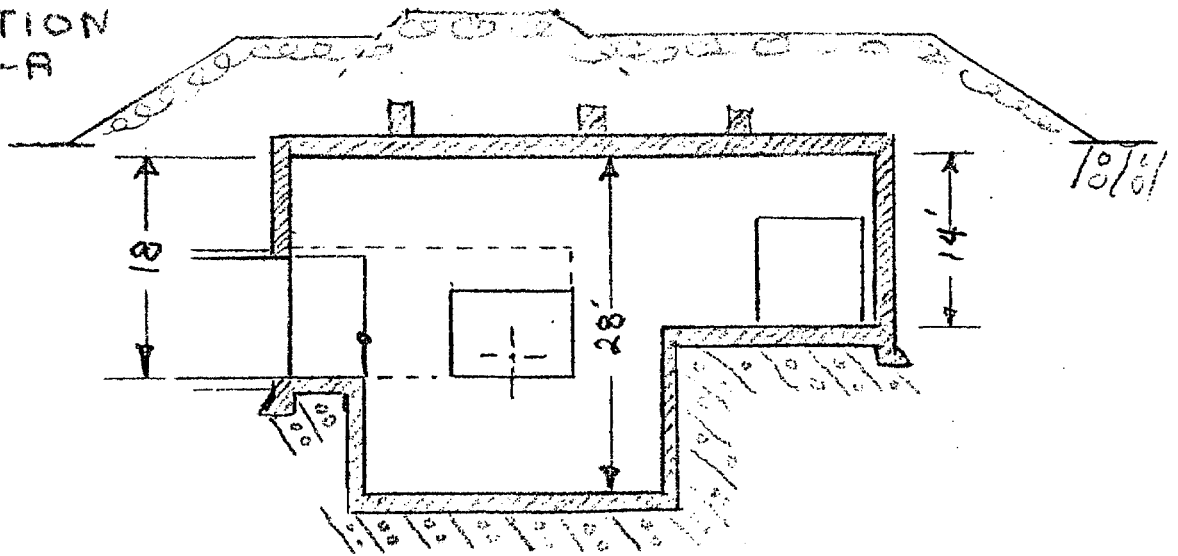
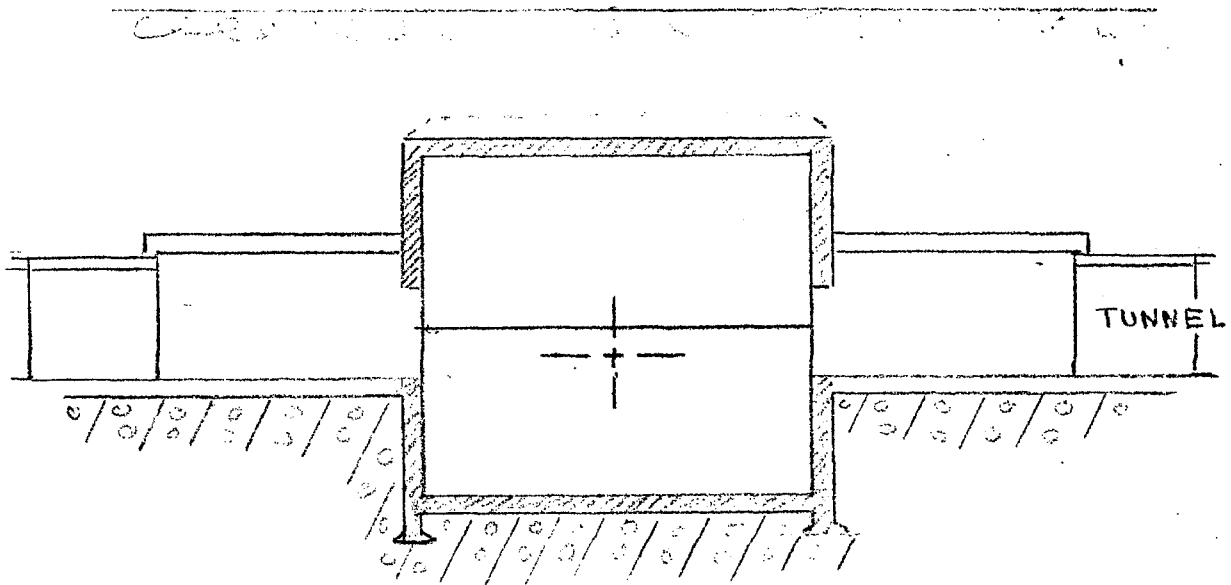


Fig. 9. COLLISION CAVE.

J&E May '76.

SECTION B-B.



SECTION C-C

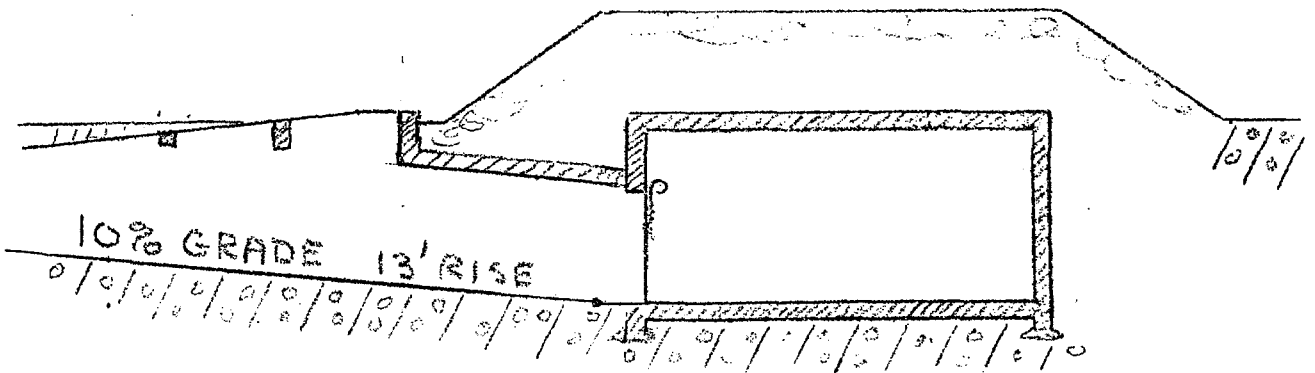


Fig.10. COLLISION CAVE.

J.P.C. May '76